06,07

Dilatometric studies of the reverse piezoelectric effect in solid solutions $(1-x)Na_{1/2}Bi_{1/2}TiO_3-xBaTiO_3$

© M.V. Gorev[1,2], S.V. Sapozhnikov[2], I.N. Flerov[1]

[1] Kirensky Institute of Physics, Federal Research Center KSC SB, Russian Academy of Sciences, Krasnoyarsk, Russia
[2] Siberian Federal University, Institute of Engineering Physics and Radio Electronics, Krasnoyarsk, Russia

E-mail: gorev@iph.krasn.ru

Received December 25, 2025
Revised December 25, 2025
Accepted December 26, 2025

Studies of the effect of a low-intensity electric field ($E < 10$ kV/cm) on the formation of the inverse piezoelectric effect in ceramic solid solutions $(1-x)Na_{1/2}Bi_{1/2}TiO_3-xBaTiO_3$ ($x = 0.05-0.97$). In the region of phase transition $Pm\bar{3}m \leftrightarrow P4mm$, ceramics with a high concentration of barium titanate are characterized by a large, close to saturation value of the normalized piezoelectric coefficient d^*_{33} ($x = 0.95$, $d^*_{33} \approx 750$ pm/V, $E = 3.3$ kV/cm). In solid solutions close in composition to the morphotropic phase boundary (MPB), the derivative $d(d^*_{33})/dE$ increases with increasing field strength. A correlation has been established between the degree of tetragonality of the crystal lattice and the behavior/values of field-induced deformation, deformation hysteresis, piezoelectric coefficient, thermal expansion, and polarization.

Keywords: phase transitions, lead-free ferroelectrics, piezoelectric effect.

DOI: 10.61011/PSS.2026.01.63246.8939-25

1. Introduction

For several decades, ferroelectric materials based on lead zirconate titanate (PZT) have established themselves as the most preferred materials for practical applications, in particular due to their high piezoelectric efficiency. However, new legally formulated environmental requirements have necessitated the replacement of lead-containing materials in the elements of functional devices of micro/nanoelectronics based on the direct or reverse piezoelectric effect, and have prompted the international scientific and technical community to search for competitive lead-free materials [1].

Significant progress has been achieved, in particular, in the study of compounds related to $BaTiO_3$ (BT) and formed upon substitution of Ba^{2+} by a combination of cations of different valences, for example $Na_{1/2}Bi_{1/2}TiO_3$ (NBT), and solid solutions $(1-x)$NBT$-x$BT, a number of properties of which allow them to be considered as promising candidates for the substitution of lead-containing materials [2–5]. Some NBT-based compounds have already demonstrated such important properties as large field-induced deformation [6], high density of stored electrical energy [7–10].

In lead-containing ferroelectric solid solutions, the most pronounced piezoelectric properties turned out to be characteristic of compounds related in the $T-x$ phase diagram to the region of the morphotropic phase boundary (MPB) between ferroelectric phases of different symmetry [11]. Based on this circumstance, researchers of lead-free solid solutions, including NBT–BT, also focused on compositions close to MPB between rhombohedral $R3c$ and tetragonal $P4mm$ phases [12].

Nevertheless, the observed piezoelectric properties of the NBT–BT system compounds cannot be considered as optimally competitive [3,13,14], since even near MPB ($x = 6-7$ %), the coefficient $d_{33} \sim 120-500$ pC/N still significantly less than, for example, for lead compounds ($d_{33} = 500-2500$ pC/N) [3].

To improve the piezoelectric properties, various modifications of the composition of solid solutions NBT–BT were also carried out by adding a third component, for example $K_{1/2}Na_{1/2}NbO_3$ (KNN) [15], and other modifiers. Noteworthy results were obtained for complex solid solutions $(1-x)Bi_{0.5}(Na_{0.8}K_{0.2})_{0.5}TiO_3-xBaTiO_3$ with $x = 0.05$ ($d^*_{33} = 630$ pm/V) [16].

Selection of a number of three-component ceramics as a research object $(1-x)$(0.8NBT–0.2BT)$-x$CaTiO$_3$ (NBT–BT–CT) [17], considered promising for use in room temperature actuators, was based on the assumption that, since the main cause of large deformations is the phase transition between nonpolar and polar states, limiting the range of concentrations of solid solutions to the MPB region does not look convincing, and the search for compounds with significant deformation potential the response induced by the electric field can be extended beyond the limits of the MPB. The ratio of components in the initial composition of 0.8NBT–0.2BT was due to the high degree of tetragonality of the structure of $P4mm$ in the concentration range near $x = 0.2$, despite the fact that in the phase diagram of $T-x$ this composition is located quite far from MPB:

$\sim$ (0.94NBT$-$0.06BT). $CaTiO_3$ was selected as the third component to reduce the depolarization temperature and achieve high field-induced deformation at room temperature. And although moderate values of macroscopic deformation were obtained, a large jump in the unit cell parameters during the field-induced phase transition indicated that compositions (NBT$-$BT$-$CT) promising for optimal electromechanical properties could well be sought far from MPB.

Despite very active studies over the years of the physical properties of solid solutions of NBT$-$BT in a wide range of component concentrations, many aspects of phase transitions and the phase diagram of $T-x$ both in the area of compositions near NBT and MPB, as well as in compositions with a high content of BT, remain unexplained so far [18–23].

Recently, we conducted detailed studies of the thermal expansion of $(1-x)$NBT$-x$BT in a wide range of concentrations and temperatures, which allowed us to clarify the specific features of the diagram $T-x$ and establish concentration regions corresponding to three groups of compounds characterized by different behavior of thermal expansion, polarization [24], dielectric constant and other properties [19,20].

The first group included solid solutions with $x > 0.40$ (region I in Figure 1). The change in BT concentration in the range of $x = 1.0-0.4$ is accompanied, firstly, by a relatively large nonlinear increase in the temperature of the ferroelectric phase transition of the first order $Pm\bar{3}m \leftrightarrow P4mm$, $T_1 = 400\,\mathrm{K}$ $(x = 1.0) \rightarrow 474\,\mathrm{K}$ $(x = 0.4)$, secondly, by increasing the degree of tetragonality c/a from 1.01 to 1.02 and, thirdly, by decreasing by $\sim 20\,\%$ the coefficient of thermal expansion of the crystal lattice β in the cubic phase.

A decrease in the concentration of barium titanate in the second group of solid solutions $(x \approx 0.40-0.15)$ (region II in Figure 1) leads to a decrease in temperature T_1 and a further decrease in the coefficient β, but the value $c/a = 1.02$ remains almost constant. At the same time, there is a gradual transformation of the ferroelectric phase transformation $Pm\bar{3}m \leftrightarrow P4mm$ from the classical type to the relaxor type, accompanied by an abnormal increase in the hysteresis of the transition temperature δT_1: from ~ 1 to 50$-$60 K.

In the third group of compounds, a further decrease of x (region III in Figure 1) is characterized by a significant increase in the temperature stability of the cubic phase (T_1^*), the appearance of successive structural distortions of two types $Pm\bar{3}m-P4bm-P4mm$ $(x = 0.06-0.15)$ and $Pm\bar{3}m-P4bm-R3c$ $(x < 0.06)$, as well as a decrease in the degree of tetragonality of the lattice in the $P4mm$ phase and the relaxor character of the structural transformations [19].

The purpose of this work is to study the inverse piezoelectric effect in NBT$-$BT solid solutions belonging to different regions of the $T-x$ phase diagrams. The nature of changes in the magnitude and temperature behavior of the deformation response of the samples as a function of the electric field strength was studied using a modified induction dilatometer. Studies of the reverse piezoelectric effect were performed on the same samples for which we previously determined the parameters of thermal expansion [24]. If necessary, this allowed for a correct joint analysis of the results of two independent experiments. The only drawback of the approach used was related to the different thicknesses of ceramic tablets $(h = 1.0-2.0\,\mathrm{mm})$, which, due to the limited voltage allowed by the dilatometer design, did not allow measurements to be carried out in the same range of electric fields for all samples.

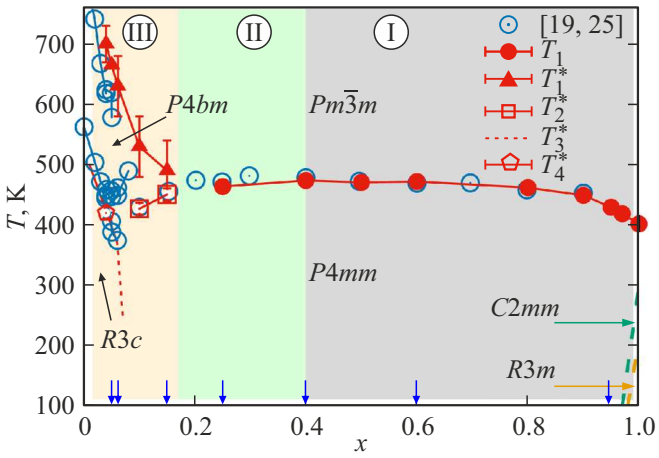

Figure 1. Concentration phase diagram of solid solutions $(1-x)$NBT$-x$BT. I, II, III — regions of BT concentrations with different behaviors of the properties of compounds [19,24,25]. The arrows on the x axis correspond to the concentrations of BT in the studied solid solutions.

2. Samples and experimental methods

Samples of solid solutions $(1-x)$NBT$-x$BT ($x = 0.95$, 0.60, 0.40, 0.25, 0.15, 0.06, 0.05), related to the three regions of the phase diagram $T-x$, in including those far from the MPB (Figure 1).

Compounds $(1-x)$NBT$-x$BT were obtained by solid-phase reaction from oxides and carbonates of high purity: TiO_2 (99.8 %), Na_2CO_3 (99.5 %), $BaCO_3$ (99.0 %) and Bi_2O_3 (99.9 %) according to the previously used methodology [19,20]. The powders of the starting materials mixed in accordance with the stoichiometric ratio were ground in an agate mortar. Depending on the composition, two-stage calcination with intermediate grinding of mixtures in a ball mill was carried out at various temperatures: from 850 °C for NBT to 1000 °C for BT and from 1000 °C (NBT) to 1150 °C (BT). The rate of heating and cooling during calcination was 3 °C/min. Then the powders crushed in an agate mortar were pressed $(p = 250\,\mathrm{MPa})$ into discs: $d = 13-15\,\mathrm{mm}$ and $h = 1.0-2.0\,\mathrm{mm}$. The pressed discs were sintered at temperatures from 1210 °C (NBT) to 1410 °C (BT). The heating and cooling rate during sintering was 2 °C/min. Calcination and sintering were carried out in

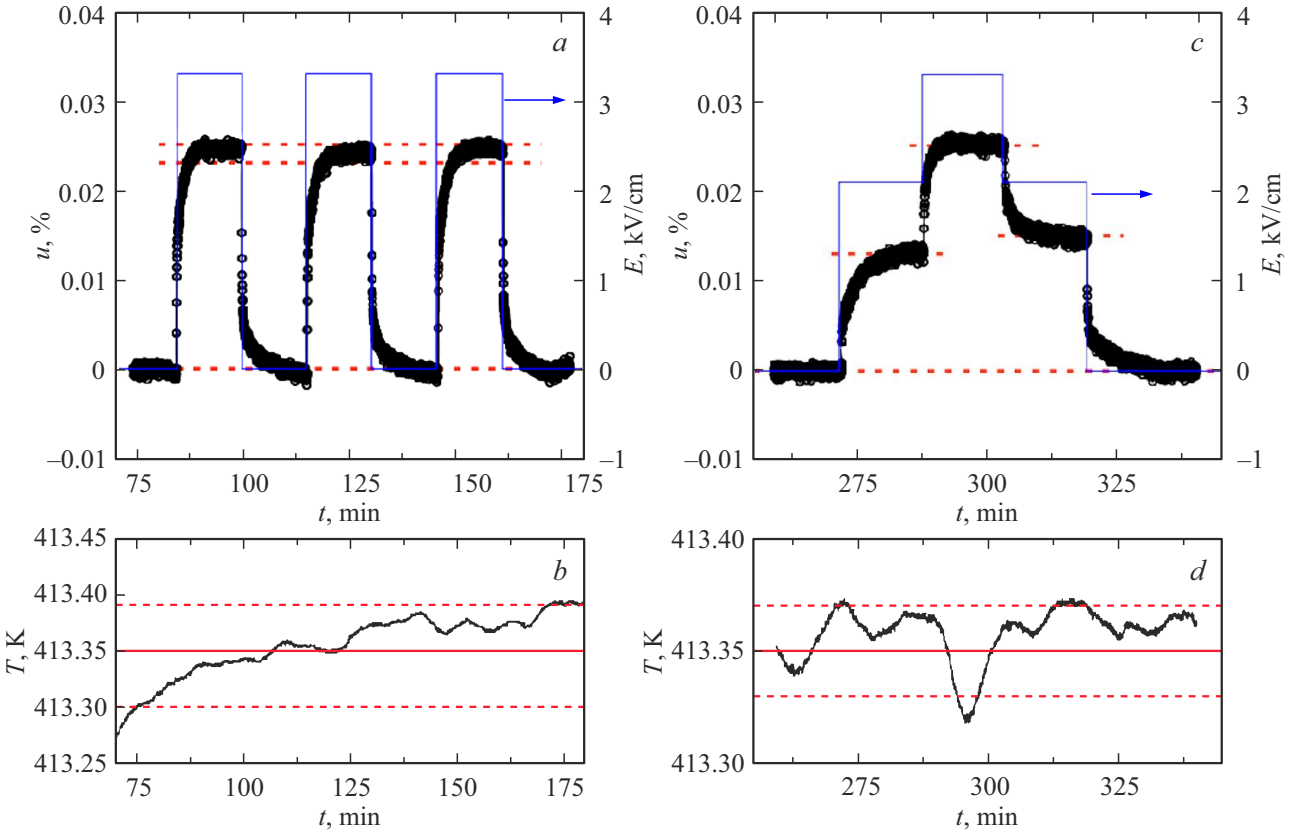

Figure 2. Behavior of deformation u of the sample with $x = 0.95$ and temperature in the measuring chamber: (a, b) at alternating field pulses of the same intensity $E = 3.3$ kV/cm, (c, d) with increasing/decreasing field strength (kV/cm) in the cycle $0 \to 2.1 \to 3.3 \to 2.1 \to 0$.

an ambient atmosphere, while no powder containing Bi was filled. The relative density of the studied samples, measured by the Archimedes method, was 94–96 %. The average grain size was practically independent of the ceramic composition and ranged from 1.5–1.6 mm.

Studies of the effect of an electric field on the deformation of ceramics were carried out in the temperature range 320–490 K using an induction dilatometer NETZSCH DIL-402C with a very high sensitivity to elongation $1.25 \cdot 10^{-10}$ m, which we previously used to study the thermal expansion of solids solutions NBT–BT [24]. Changes were made to the dilatometer design, which made it possible to simultaneously measure both the temperature dependences of thermal expansion and the deformation response of the sample to changes in the external electric field, that is, the reverse piezoelectric effect. Silver electrodes were applied to the surface of the samples by vacuum sputtering to study the deformation in an electric field. The copper wires were connected to the electrodes with a conductive silver paste.

The voltage applied to the electrodes varied in the range of 0–1 kV using a stable high-voltage source. Depending on the thickness of the samples, the maximum electric field strength did not exceed $E_{max} = 5–10$ kV/cm, which was due to two reasons. On the one hand, the design features of the dilatometer did not allow the use of higher voltages, and on the other hand, a decrease in the thickness of the sample would inevitably lead to an increase in the error in determining the deformation caused, among other things, by a violation of the flatness of the thin sample when the field is turned on/off (bending) [26].

3. Results and discussion

Figure 2 shows the time dependences of the electric field strength, the linear deformation response $u = \Delta L/L$ associated with the inverse piezoelectric effect, and temperature changes in the measuring chamber during studies of a solid solution with $x = 0.95$ in the tetragonal phase $P4mm$ at $T_1 - T = 16$ K, which are qualitatively consistent with the results obtained for other NBT–BT samples studied in the paper.

A high reproducibility of the behavior of deformation u was observed with repeated field pulses lasting 15 min (Figure 2, a). Depending on the value of E and the proximity/remoteness of the temperature range of the individual experiment from the temperature of the phase transition, the error in determining u was about $\pm(2–5)$ %. It is quite possible to speak about a rather high degree of isothermicity

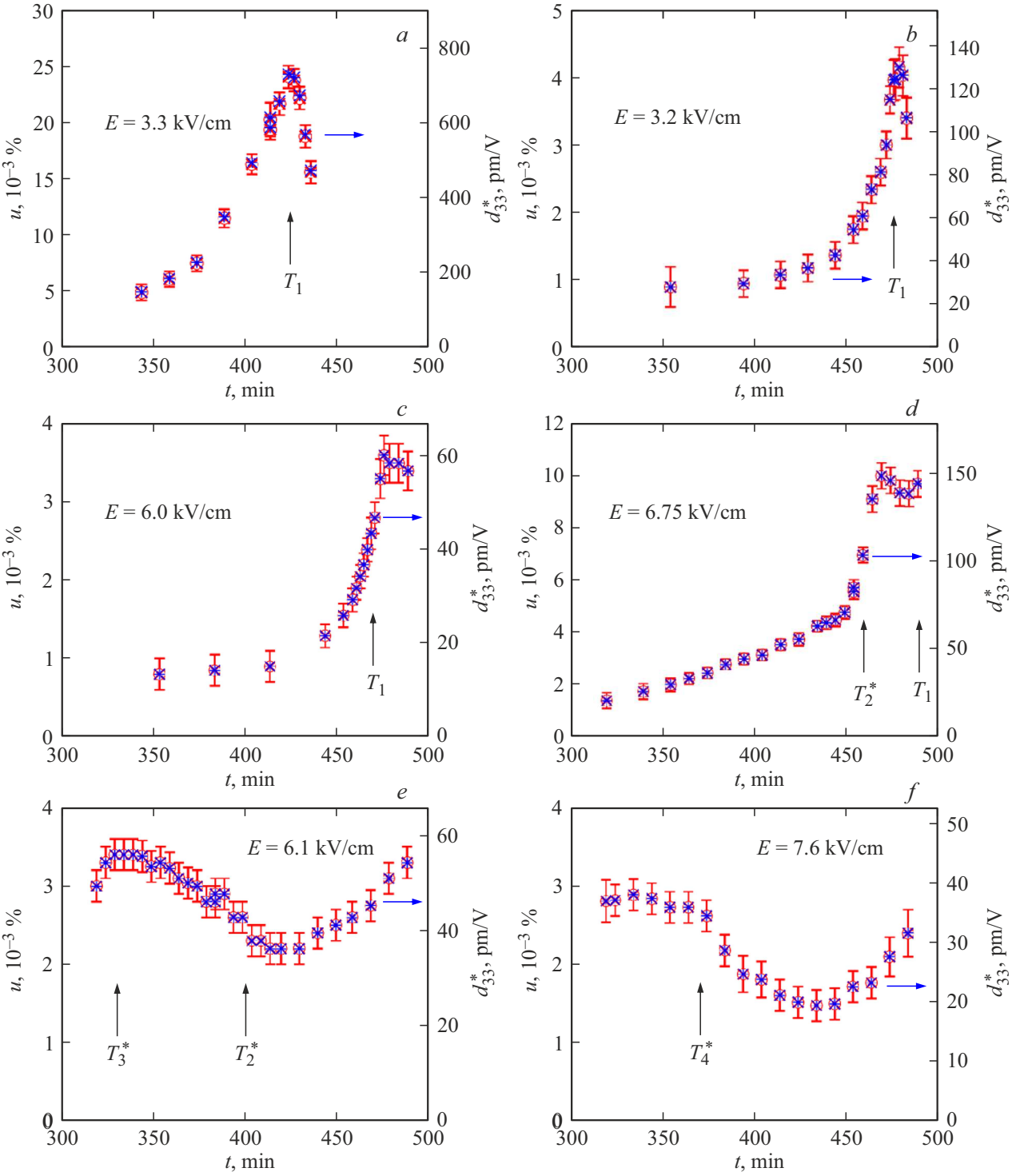

Figure 3. Temperature dependences of deformation u and piezoelectric coefficient d_{33}^* of solid solutions of $(1-x)$NBT–xBT with $x = 0.95$ (*a*), 0.40 (*b*), 0.25 (*c*), 0.15 (*d*), 0.06 (*e*) and 0.05 (*f*). The temperatures T_1, T_1^*, T_2^*,T_3^*, T_4^* correspond to the phase boundaries in the diagram $T-x$ (Figure 1).

of the measurement processes, since for any variation of the field strength, temperature fluctuations did not exceed $\pm(0.02-0.04)$ K (Figure 2). Due to the relatively small value of the coefficient of linear thermal expansion of ceramic samples NBT–BT ($\alpha \approx 10^{-5}\,\mathrm{K}^{-1}$ [24]), the contribution to the uncertainty of the measured deformation due to the indicated temperature drift was extremely insignificant $\sim(\pm 10^{-4}\,\%)$. There was no correlation in time between temperature fluctuations and switching on/off the field (Figure 2), which indicated the absence of any

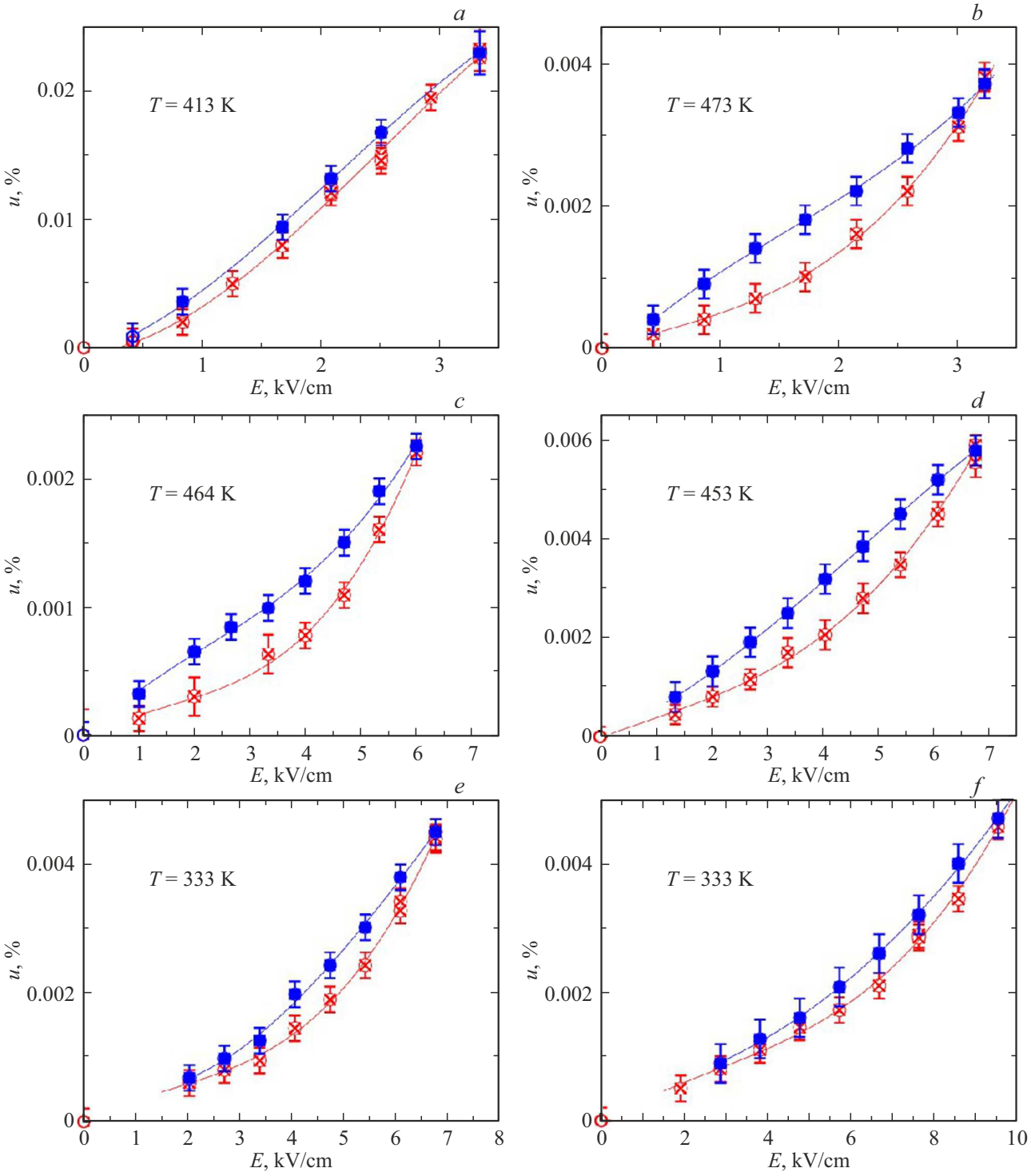

Figure 4. Unipolar hysteresis loops $u-E$ of solid solutions of $(1-x)$NBT$-x$BT with $x = 0.95$ (*a*), 0.40 (*b*), 0.25 (*c*), 0.15 (*d*), 0.06 (*e*), 0.05 (*f*).

significant heat generation in the sample due to the Joule effect and/or the electrocaloric effect.

The dependencies $[u(E)]_T$ were also studied with a two-stage increase in the field to the maximum $(0 \to E_1 \to E_2)$ followed by a decrease to the initial value $(E_2 \to E_1 \to 0)$ (Figure 2, *c*). The latter procedure allowed us to observe hysteresis phenomena, expressed in a mismatch of u values at the same field E_1, implemented in the processes of increasing $(0 \to E_1)$ and decreasing $(E_2 \to E_1)$ field strength.

Figure 3, *a* and 3, *b* show the temperature dependences of the field-induced deformation of u at $E = \text{const}$ in solid

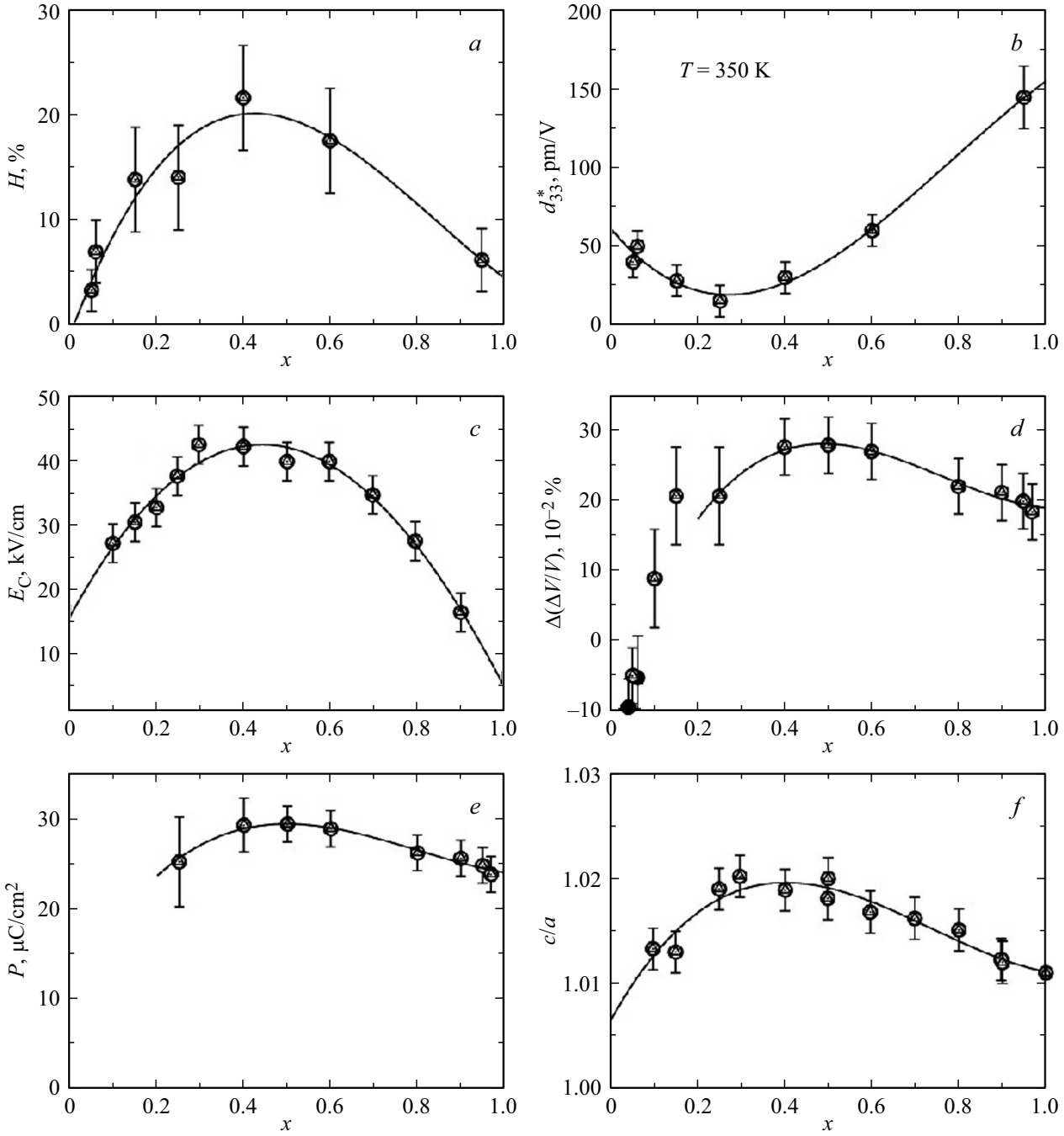

Figure 5. Effect of BT concentration on the properties of solid solutions NBT−BT at 350 K: *a* — relative hysteresis H of unipolar loops $u-E$; *b* — piezoelectric coefficient d^*_{33}; *c* — coercive field E_C [19,24]; *d* — abnormal volumetric deformation in saturation (at 100 K); *e* — RMS polarization P [24]; *f* — degree of tetragonality c/a of the crystallographic cell in the $P4mm$ phase.

solutions with $x = 0.95$ and 0.40 (region I of the phase diagram $T-x$) undergoing a transition from the cubic $Pm\bar{3}m$ phase to the ferroelectric tetragonal phase $P4mm$. The same graphs show the temperature dependences of the normalized strain coefficients $d^*_{33} = u/E$.

In addition to the previously mentioned features in the physical properties of NBT−BT, depending on the concentration of BT [24], the change in x from 0.97 to 0.40 is accompanied by two more circumstances. Firstly, there is a decrease in the maximum values of the functions $[u(T)]_E$ and $d^*_{33}(T)$ and, secondly, the corresponding temperatures $T_u^{\max}$ increase relative to the transition temperature in the absence of an electric field, $T_1^{E=0}$, with a small fast $dT_u^{\max}/dE \approx 1\,\mathrm{K}\cdot(\mathrm{kV/cm})^{-1}$. In solid solutions with $x < 0.4$, characterized either by a mixture of phases or by relaxor behavior (regions II and III in Figure 1) [21], the difference between these temperatures increases significantly (Figure 3, *c–f*), and maximum values of d^*_{33}, weakly

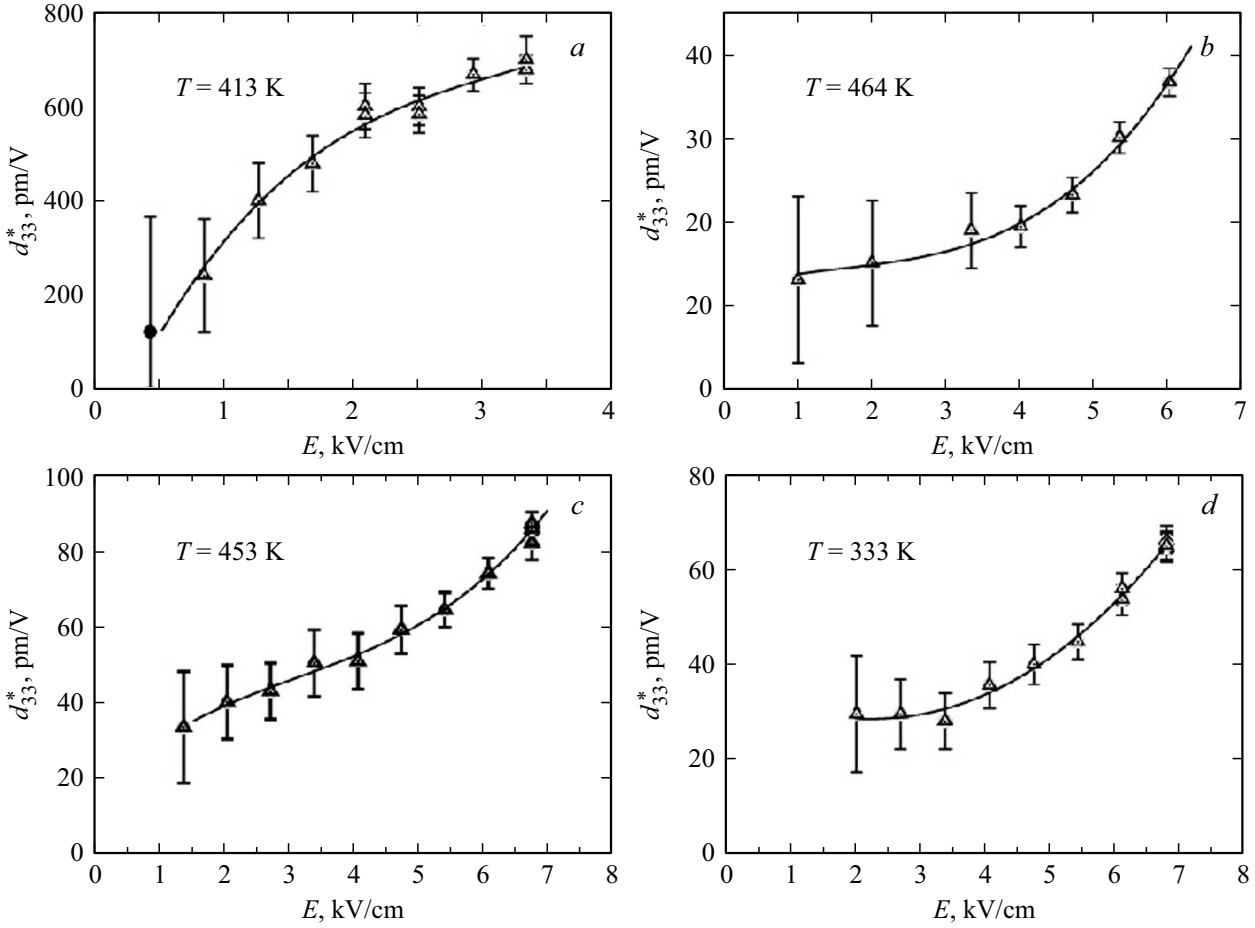

Figure 6. Dependence of the piezoelectric coefficient d^*_{33} on the electric field for solid solutions of $(1-x)$NBT–xBT with $x = 0.95$ (*a*), 0.25 (*b*), 0.15 (*c*), 0.06 (*d*).

dependent on temperature, are observed in samples with $x = 0.06$ and 0.05 (Figure 3, *e* and 3, *f*), close to MPB.

For all the solid solutions studied in the work, the deformation behavior in isothermal modes of increasing/decreasing electric field strength was determined and, thus, unipolar hysteresis loops u–E were obtained (Figure 4). Since deformation changes reach large values near phase transitions, measurements were carried out precisely in these areas of distorted phases ($P4mm$ — $x = 0.95$; 0.60; 0.25; 0.15; $R3c$ — $x = 0.06$; 0.05), remote from the temperatures of the corresponding structural transformations at $T_i - T \approx 6$–15 K.

It should be noted that the maximum electric fields used in the experiments under consideration, $E_{\max} < 10$ kV/cm, are lower than the coercive fields, $E_C = 20$–40 kV/cm [19], which does not allow the hysteresis loops to be fully deployed and P–E, and u–E. In addition, the dependences $P(E)$ and $u(E)$ are measured, as a rule, at high frequencies of the alternating field $f > 0.1$ Hz. In our case, pulses with a duration of ~ 10–15 min were used. During this time, the domain structure manages to return almost to an equilibrium state and the hysteresis measured by us turns out to be less than with measurements in an alternating field.

The relative strain hysteresis is defined as $H = (u_- - u_+)E_{\max/2}/u_{\max}$, where u_+ and u_- are deformations on the ascending and descending branches of the hysteresis loop corresponding to half of the maximum field $E_{\max}$ [27]. The value of H varies significantly depending on the concentration of BT (Figure 5, *a*), reaching a maximum of $\sim 20\,\%$ at the boundary of the I and II groups of solid solutions and decreasing to $\sim 5\,\%$ in compounds of group III ($x = 0.06$, 0.05), in which the relaxor behavior was observed [28].

Figure 5 shows the concentration dependences of other equally important characteristics of solid solutions: the piezoelectric coefficient d^*_{33} (extrapolated to 350 K), the coercive field E_C [19], as well as the anomalous deformations in saturation at 100 K and RMS polarization [24]. It can be seen that the behavior of all the presented physical properties, with the exception of the coefficient d^*_{33}, is almost identical and quite satisfactorily corresponds to the behavior of the tetragonal degree c/a of the crystallographic cell in the phase $P4mm$ (Figure 5, *f*) [19]. The behavior of d^*_{33} observed in low-intensity fields, $E \ll E_C$, is due to the fact that an increase and subsequent decrease in the value of c/a with a decrease in BT concentration is accompanied by

a faster increase/decrease in the coercive field compared with reverse piezoelectric deformation. If the fields are larger than coercive, this dependency may change.

In solid solutions belonging to the concentration range of $0.2 < x < 0.4$, a wide temperature range of phases $P4mm$, $P4bm$, $Pm\bar{3}m$ [28] was observed, which, as we approach $x = 0.2$ led to a gradual decrease in the deformation and polarization observed in the experiment [24]. Moreover, in the $P4bm$ phase, in addition to the displacement of the titanium ion from the center of the octahedron, the octahedra rotate, accompanied by the appearance of deformation and polarization of the opposite sign [29–31] and, as a result, a decrease in the total values of u and P. An electric field greater than the critical one (~ 20 kV/cm in composition with $x = 0.07$) suppresses octahedral rotations and induces a transition from $P4bm$ to $P4mm$ with a significant increase in deformation, polarization, and piezoelectric coefficient [29,30]. Unfortunately, the maximum electric field used in the operation (5−10 kV/cm) is insufficient to induce a phase transition between $P4mm$ and $P4bm$.

Figure 6 shows the isothermal dependences of the piezoelectric coefficient d^*_{33} on the electric field for a number of solid solutions of $(1-x)$NBT−xBT from various regions of the phase diagram $T-x$.

It can be seen that the value d^*_{33} is close to saturation at low-intensity fields (Figure 6, a) for a composition close to $BaTiO_3$, for which the coercive field is small, $E_C < 10$ kV/cm [19] (Figure 5, c). In solid solutions similar in composition to NBT, the coercive field is large $\sim 25-40$ kV/cm [19] (Figure 5, c) and the coefficient d^*_{33} is significantly lower, however, its change with increasing field is characterized by an increasing derivative $d(d^*_{33})/dE$ (Figure 6, $b-d$). The latter result is consistent with the data from the study of the reverse piezoelectric effect in a solid solution of 0.8NBT−0.2BT: at the same distance from the phase transition temperature $Pm\bar{3}m \leftrightarrow P4mm$, T_1 — 50 K, the value of d^*_{33} — 200 pm/V at $E = 65$ kV/cm [17] turns out to be an order of magnitude higher than $d^*_{33} \approx 17$ pm/V for the studied by us and similar in composition 0.75NBT−0.25BT ($E = 6$ kV/cm) (Figure 3).

4. Conclusion

Studies of the inverse piezoelectric effect in ceramics $(1-x)$NBT−xBT ($x = 0.05-0.97$) over a wide temperature range have been performed. The experiments were carried out using an upgraded induction dilatometer on the same samples that we had previously used to study the thermal expansion [24]. The dilatometer design provided for limiting the electrical voltage applied to the samples in the measuring chamber, $U < 1$ kV, as a result of which measurements of the deformation response were carried out in electric fields $E < 10$ kV/cm. However, this circumstance can certainly be considered as positive for two reasons. First, this limitation stimulated the acquisition of original experimental information about the nature and features of the formation of parameters of the inverse piezoelectric effect (d^*_{33}, strain hysteresis) in low-intensity fields in samples with compositions close to and far from MPB. And, secondly, the results obtained will be of undoubted interest to specialists in the field of functional piezoelectric devices operating in an ambient atmosphere and preventing the possibility of placing a piezoelectric element in an oil bath used to avoid breakdown at high field strength.

It has been found that when the temperature and concentrations of the components of solid solutions $(1-x)$NBT−xBT vary, the piezoelectric coefficient values in electric fields with a voltage less than corresponding to coercive fields vary in the range from 30 to ~ 750 pm/V and are comparable with coefficients typical for other lead-free piezoelectric materials with significantly higher field strength [3,13,14].

It was found that in solid solutions of $(1-x)$NBT−xBT with a high concentration of BT, the value of the normalized strain coefficient d^*_{33} in the phase transition region fully corresponds to its values observed in ceramics close to MPB, but in stronger fields. However, for a sample with $x = 0.95$, the large value $d^*_{33} \approx 750$ pm/V is close to saturation already at $E = 3.3$ kV/cm, while in solid solutions with $x < 0.8$ the derivative $d(d^*_{33})/dE$ increases with increasing field strength (Figure 6).

An analysis of the data obtained together with the results of previous studies [19,20,24] showed that the possibility of dividing the system of solid solutions with $x = 0.04-1.00$ into three groups, discovered during the study of thermal expansion under conditions of $E = 0$ (Figure 1, [24]) fully applies to the temperature/concentration dependences of field-induced deformation, strain hysteresis, coefficient d^*_{33}, coercive field and polarization. The established correlation in the behavior of different physical properties with varying BT content is consistent with the nature of the change in the degree of tetragonality of the crystal cell in the phase $P4$ [19] (Figure 5).

Acknowledgments

Dilatometric data were obtained on the equipment of the Krasnoyarsk Regional Center for Collective Use of the Federal Research Center — Krasnoyarsk Scientific Center of the Siberian Branch of the Russian Academy of Sciences.

Funding

The study was carried out within the framework of the research topic of the State Assignment of the Institute of Physics of the Siberian Branch of the Russian Academy of Sciences.

Conflict of interest

The authors declare that they have no conflict of interest.

References

[1] H.C.H. Hofmann, G.C. Rowe, A. Türk. Administrative Law and Policy of the European Union. Oxford University Press (2011), 3–20.
[2] J. Wu, H. Zhang, C.-H. Huang, C.-W. Tseng, N. Meng, V. Koval, Y.-C. Chou, Z. Zhang, H. Yan. Nano Energy **76**, 105037 (2020).
[3] J. Hao, W. Li, J. Zhai, H. Chen. Mater. Sci. Eng. R Rep. **135**, 1 (2019).
[4] M. Acosta, N. Novak, V. Rojas, S. Patel, R. Vaish, J. Koruza, G.A. Rossetti, J. Rödel. Appl. Phys. Rev. **4**, 041305 (2017).
[5] F. Wang, C. Zhu, S. Zhao. J. Alloys Compd. **869**, 159366 (2021).
[6] J. Chen, Y. Wang, L. Wu, Q. Hu, Y. Yang. J. Alloys Compd. **775**, 865 (2019).
[7] F. Gao, X. Dong, C. Mao, W. Liu, H. Zhang, L. Yang, F. Cao, G. Wang. J. Am. Ceram. Soc. **94**, 4382 (2011).
[8] W. Shi, L. Zhang, R. Jing, Y. Huang, F. Chen, V. Shur, X. Wei, G. Liu, H. Du, L. Jin. Nanomicro Lett. **16**, 91 (2024).
[9] T. Li, X. Yang, Q. Cheng, A. Xie, X. Jiang, C. Zhou, Y. Zhang, R. Zuo. J. Alloys Compd. **970**, 172524 (2024).
[10] R. Lang, Q. Chen, T. Gao, J. Zhu, J. Xing, Q. Chen. J. Eur. Ceram. Soc. **44**, 3916 (2024).
[11] B. Noheda, D. Cox, G. Shirane, R. Guo, B. Jones, L. Cross. Phys. Rev. B **63**, 014103 (2001).
[12] M. Chen, Q. Xu, B.H. Kim, B.K. Ahn, J.H. Ko, W.J. Kang, O.J. Nam. J. Am. Ceram. Soc. **28**, 843 (2008).
[13] J. Rödel, W. Jo, K.T.P. Seifert, E.-M. Anton, T. Granzow, D. Damjanovic. J. Am. Ceram. Soc. **92**, 1153 (2009).
[14] T. Takenaka, H. Nagata, Y. Hiruma. Japan. J. Appl. Phys. **47**, 37874 (2008).
[15] S.-T. Zhang, A.B. Kounga, E. Aulbach, W. Jo, T. Granzow, H. Ehrenberg, J. Rödel. J. Appl. Phys. **103**, 034108 (2008).
[16] P. Jaita, P. Jarupoom. J. Asian Ceram. Sci. **9**, 975 (2021).
[17] M. Jurjans, L. Bikse, E. Birks, Š. Svirskas, M. Antonova, M. Kundzins, A. Sternberg. AIP Adv. **12**, 035124 (2022).
[18] Y. Yao, Z. Sun, Y. Ji, Y. Yang, X. Tan, X. Ren. STAM **14**, 035008 (2013).
[19] M. Dunce, E. Birks, M. Antonova, A. Plaude, R. Ignatans, A. Sternberg. Ferroelectrics **447**, 1 (2013).
[20] A. Plaude, R. Ignatans, E. Birks, M. Dunce, M. Antonova, A. Sternberg. Ferroelectrics **500**, 47 (2016).
[21] L.S. Kamzina, I.P. Pronin. FTT **65**, *9*, 1566 (2023) (in Russian).
[22] G. Picht, J. Toopfer, E. Henning. J. Eur. Ceram. Soc. **30**, 3445 (2010).
[23] K. Datta, P.A. Thomas, K. Roleder. Phys. Rev. B. **82**, 224105 (2010).
[24] M. Gorev, I. Flerov, M. Molokeev, K. Bormanis, E. Birks, S. Sapozhnikov, E. Mikhaleva. J. Eur. Ceram. Soc. **44**, 116769 (2024).
[25] F. Cordero, F. Craciun, F. Trequattrini, E. Mercadelli, C. Galassi. Phys. Rev. B. **81**, 144124 (2010).
[26] G. Das Adhikary, A. Adukkadan, G.J. Muleta, Monika, R.P. Singh, D.N. Singh, H. Luo, G.A. Tina, L. Giles, S. Checchia, J. Daniels, R. Ranjan. Nature **637**, 333 (2025).
[27] M.D. Nguyen, E.P. Houwman, G. Rijnders. Sci. Rep. **7**, 12915 (2017).
[28] G. Das Adhikary, B. Mahale, B.N. Rao, A. Senyshyn, R. Ranjan. Phys. Rev. B. **103**, 184106 (2021).
[29] Y. Kitanaka, K. Hirano, M. Ogino, Y. Noguchi, M. Miyayama, C. Moriyoshi, Y. Kuroiwa. Sci. Rep. **6**, 32216 (2016).
[30] Y. Kitanaka, M. Ogino, K. Hirano, Y. Noguchi, M. Miyayama, Y. Kagawa, C. Moriyoshi, Y. Kuroiwa, S. Torii, T. Kamiyama. Jap. J. Appl. Phys. **52**, 09KD01 (2013).
[31] Y. Kitanaka, M. Ogino, Y. Noguchi, M. Miyayama, A. Hoshikawa, T. Ishigaki. Jap. J. App. Phys. **57**, 11UD05 (2018).

Translated by A.Akhtyamov